High-Energy Photoproton Production by 325-Mev Bremsstrahlung Radiation*

B. T. Feld, R. D. Godbole,† A. Odian, F. Scherb, P. C. Stein, and A. Wattenberg
Physics Department and Laboratory for Nuclear Science, Massachusetts Institute of Technology, Cambridge, Massachusetts
(Received February 8, 1954)

Photoprotons with energies above 120 Mev have been studied at the M.I.T. synchrotron. Angular distributions of protons with 126 Mev, 169 Mev, and 203 Mev were obtained in the angular range from 20° to 160° from both beryllium and carbon targets. These observations showed that the protons in a Be and in a C nucleus behave identically in high energy photoproton production. The energy distribution of photoprotons from carbon at 30° was investigated in particular detail. A break is observed in the energy distribution which appears to be in accordance with Levinger's "quasi-deuteron model." Absolute values for the differential and total cross sections were obtained.

A detailed analysis of existing data is given which raises the possibility that the agreement with the "quasi-deuteron model" may be fortuitous.

I. INTRODUCTION

AMONG the products of the reactions of γ rays with nuclei, protons have been observed and studied by many investigators.[1] For γ rays of energy between the threshold ($\sim$5–8 Mev) and $\sim$50 Mev, most of the photoprotons arise from the absorption of the γ ray in a "dipole resonance" reaction, followed by the evaporation of a proton from an excited compound nucleus.

However, even in the dipole resonance energy range, an appreciable fraction of the proton emission results from a direct interaction between the γ ray and one of the protons in the nucleus.[2,3] These directly emitted photoprotons exhibit two characteristic features (1) they carry away a large fraction of the incident γ-ray energy, and (2) their angular distribution, unlike that of the evaporation protons, is not isotropic, but tends to exhibit the $\sin^2\theta$ distribution characteristic of a photoelectric ejection process.[3,4]

At higher energies, photon absorption usually results in multiple particle emission.[5,6] The energy dependence of the cross section for photon absorption in the energy range $\sim$50–150 Mev is not yet well established but, once the dipole resonance has been passed, the cross section appears to be small and either slowly decreasing or more-or-less flat with increasing energy. In the region of $\sim$140 Mev, which corresponds to the onset of the possibility of π-meson production, the cross section for photon absorption appears to increase. Most absorptions result in "stars," and the increase in cross section is believed to be meson-connected.[7,8] However, in moderately heavy nuclei, a large fraction of the mesons produced may be reabsorbed in the same nucleus, giving rise to the evaporation of a number of neutrons, protons, α particles, and possibly heavier nuclear fragments.[8]

Also, at the higher photon energies, the γ ray frequently ejects a proton of energy comparable to that of the incident photon. The most direct way of studying this process is to observe the high-energy protons emitted from targets bombarded by high-energy x-rays.[9] Such observations are not easy to interpret unambiguously, since the bremsstrahlung spectrum falls off rapidly with increasing energy, so that the resulting proton spectrum represents an integral in which the effects of the lower-energy photons are strongly weighted.

Nevertheless, a considerable amount of information is available as a result of a number of investigations of the high-energy photoprotons from x-rays on various targets. Levinthal and Silverman,[10] using the 322-Mev x-ray beam from the Berkeley Synchrotron, studied the protons of energies between 10 and 70 Mev. They obtained proton energy spectra falling off with energy roughly as E^{-2}. The 10-Mev protons were emitted isotropically; these are probably the tail of the evaporation spectra. The 40-Mev protons, on the other hand, showed a distinct forward peaking. Walker[11] studied the protons of energy $\gtrsim$70 Mev at a number of angles from a carbon target bombarded by a 195-Mev x-ray beam from the Cornell synchrotron. He found a forward peaking in the angular distribution and a rapid decrease with energy $\sim E^{-5}$ in the integral proton spectrum.

Keck,[12] at Cornell, expanded and extended the ob-

* This work was supported in part by the joint program of the U. S. Office of Naval Research and the U. S. Atomic Energy Commission.

† Now at Ramnarain Ruia College, Bombay, India.

[1] For a summary of work up to 1952, see K. Strauch, Ann. Rev. Nuclear Sci. **2**, 105 (1953).

[2] O. Hirzel and H. Wäffler, Helv. Phys. Acta **20**, 373 (1948).

[3] E. D. Courant, Phys. Rev. **82**, 703 (1951).

[4] P. R. Byerly, Jr., and W. E. Stephens, Phys. Rev. **83**, 54 (1951).

[5] K. Strauch, Phys. Rev. **81**, 973 (1951).

[6] Debs, Eisinger, Fairhall, Halpern, and Richter (private communication).

[7] R. D. Miller, Phys. Rev. **82**, 260 (1951).

[8] S. Kikuchi, Phys. Rev. **80**, 492 (1950); **83**, 1255 (1951); **86**, 41 (1952).

[9] In the energy range under discussion, the only available sources of appreciable intensity are bremsstrahlung sources. J. W. Weil and B. D. McDaniel [Phys. Rev. **92**, 391 (1953)] have developed a method of making observations with monochromatic photons which, owing to the very small available intensities, is of rather limited applicability.

[10] C. Levinthal and A. Silverman, Phys. Rev. **82**, 822 (1951).

[11] D. Walker, Phys. Rev. **81**, 634 (1951); **84**, 149 (1951).

[12] J. C. Keck, Phys. Rev. **85**, 410 (1952).

servations on the high-energy photoprotons from 300-Mev x-rays to proton energies of ~200 Mev and over a wider range of angles and target elements. He found that the cross section for photoproton ejection increased linearly with atomic number; that the angular distributions became more sharply peaked forward with increasing energy; and that the proton energy spectra showed a sharp break in slope at an energy of approximately half of the maximum photon energy (e.g., at 67.5° to the beam, the proton energy distribution changed from E^{-2} to E^{-6} at ~130 Mev).

This last feature gave rise to the suggestion, developed theoretically by Levinger,[13] that the energetic photoprotons result from the direct interaction of photons with deuteron-like sub-units in the nucleus. Subsequent measurements, by Rosengren and Dudley,[14] with the 322-Mev x-rays from the Berkeley synchrotron, by Perry and Keck,[15] who employed a subtraction technique to obtain the effect of monochromatic γ rays, and by Weil and McDaniel,[16] using monochromatic 190-Mev γ rays,[9] as well as by the present authors,[17] have tended to confirm and further elucidate the main features of the photoproduction process suggested by the work of Keck.[12]

However, the "deuteron model," as developed by Levinger,[13] is not nearly as successful in accounting for other features of the high-energy photoproton distributions. In particular, the observed angular distributions appeared to be much more strongly peaked in the forward direction than predicted.

The experiments herein reported were undertaken in an attempt to further clarify the nature of the high-energy photoproton production process. While in many respects they cover the same ground as investigations

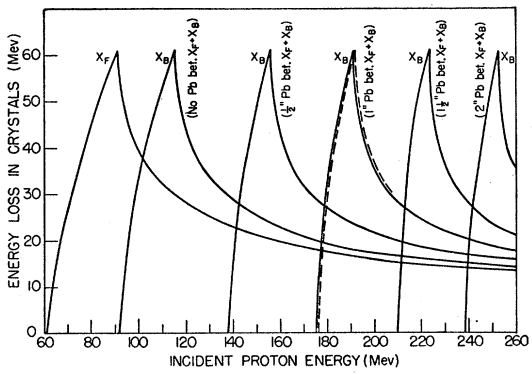

FIG. 1. Proton energy loss in 5.1 g/cm² NaI crystals *versus* the incident proton energy. All curves are for a $\frac{1}{4}$-in. Pb absorber in front of the crystals. The X_F curve is for the energy loss in the front crystal. The X_B curves are for the back crystal. The dotted curve is for a total absorber of $1\frac{1}{4}$ in. of Pb placed in front of the first crystal.

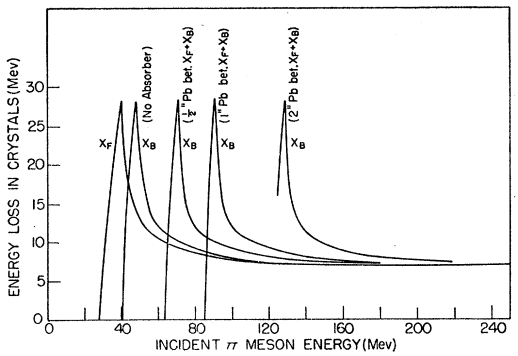

FIG. 2. π meson energy loss in 5.1 g/cm² NaI crystals *versus* the incident π meson energy. All curves are for a $\frac{1}{4}$-in. Pb absorber in front of the crystals. The X_F curve is for the energy loss in the front crystal. The X_B curves are for the back crystal.

previously reported,[12,14] they have extended these investigations both in energy and in angle, and have attempted to provide a quantitative basis for comparison with theory. In the majority of these investigations a carbon target was employed; however, several other elements were also studied.

II. METHOD OF OBSERVATION

Our method of proton detection is essentially the same as that described by previous investigators.[12,14] However, it differs in a sufficient number of significant details so that a brief description of the main features may be in order.

The protons were detected, and distinguished from other charged particles, by observation of the pulse heights in the two crystals of a scintillation counter telescope. Both crystals usually were about $\frac{5}{8}$ in. thick and 4 in. in diameter. NaI:Tl crystals were used to obtain a linear relation between pulse height and energy loss in the crystal. End-window (5819) photomultipliers viewed the crystals at a distance of a few inches in order to increase the uniformity of the light collection from different regions of the crystal. The method of proton energy discrimination may be understood most easily by reference to Fig. 1, which is a plot of the proton ionization energy loss in each of the crystals as a function of the energy of the protons incident on the telescope. The first curve, labeled X_F, shows the proton energy loss in the front crystal while the succeeding curves, X_B, show the proton energy loss in the back crystal for various thicknesses of lead absorber placed between the two crystals. In Fig. 2 are plotted the corresponding ionization energy losses for π mesons. The energy loss data, on which these curves are based, were taken from the compilation of Aron, Hoffman, and Williams.[18]

The detection of protons of a given energy E_0 is accomplished as follows: The approximate thickness of absorber, such that the peak of the energy loss in X_B

[13] J. S. Levinger, Phys. Rev. **84**, 43 (1951).
[14] J. W. Rosengren and J. M. Dudley, Phys. Rev. **89**, 603 (1953).
[15] A. M. Perry and J. C. Keck, Phys. Rev. **86**, 629 (1952).
[16] J. W. Weil and B. D. McDaniel, Phys. Rev. **92**, 391 (1953).
[17] Wattenberg, Feld, and Godbole, Phys. Rev. **90**, 380 (1953).
[18] Aron, Hoffman, and Williams, Atomic Energy Commission Report AECU-663, UCRL-121, 1949 (unpublished).

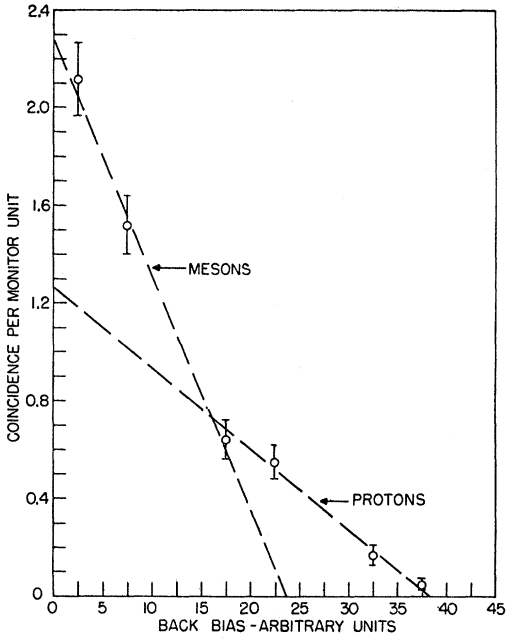

FIG. 3. Coincidence counting rate as a function of the bias on the back crystal. The front bias is set at a value slightly below the value at which protons should be counted. The straight lines are drawn on the assumption that the upper portions of the curves in Figs. 1 and 2 can be approximated by triangles.

(Fig. 1) falls at E_0, is inserted in the telescope. A curve is then taken of the coincidence telescope counting rate as a function of the bias setting (proportional to the minimum pulse height) on the back crystal. While taking this curve, the bias on the front crystal is set rougly somewhat below the value at which protons should be counted, but, if possible, above the value corresponding to the energy loss of a particle at the minimum of its ionization. An example of such an integral "back-bias" curve is shown in Fig. 3. From this curve, the value of the bias setting corresponding to 61 Mev (the peak of the proton energy loss curve) is determined. The back bias is then set to a somewhat lower value such as to make the proton energy resolution as sharp as possible consistent with a reasonable counting rate, i.e., about 45 Mev. In the case of the data to be discussed, the proton energy spread was kept below 15 percent in all cases.

Once this bias setting for the back crystal has been decided, the proper bias setting for the front crystal is determined by taking integral bias curves of the type illustrated in Fig. 4. These curves demonstrate a number of characteristics of our detection technique. It may be noted that above the plateau region, the counting rate falls off with increasing bias over a finite range. In practice, the width of this "fall-off" region is not primarily determined by instrumental factors. Rather, this width is determined by the variation of proton energy loss in the front crystal over the finite range of proton energies accepted by the back crystal. It is seen from Fig. 1 that the width of the "fall-off" region should decrease with increasing absorber thickness, as indeed it does. The width of the break in the front crystal bias curves provides another check on our calibration of the energy resolution of the telescope. In normal operation, the bias of the front crystal is set at a value slightly below that of the "break," so as to count all the protons accepted by the back crystal while, at the same time, minimizing the possibility of counting mesons by setting as far as possible above the bias corresponding to the energy loss in the front crystal of mesons stopping in the back crystal (see Fig. 2).

Another feature of the curves of Fig. 4 is the fact that the bias at which the break occurs decreases with increasing absorber thickness when the absorber is placed between the crystals. This is, again, as expected from consideration of the curves of Fig. 1, and provides an additional check on the calibration of the counter telescope. Actually, this feature represents one of the disadvantages of our detection scheme, since it means that a new calibration curve must be run and a new front crystal bias setting must be determined for each absorber thickness used. (The calibration of the back crystal, however, is independent of the absorber thickness, although the energy resolution, for a given bias setting, changes with absorber thickness.) This difficulty can be overcome by placing the absorber in front of the telescope rather than between the crystals. Curves of energy loss *vs* incident proton energy, corre-

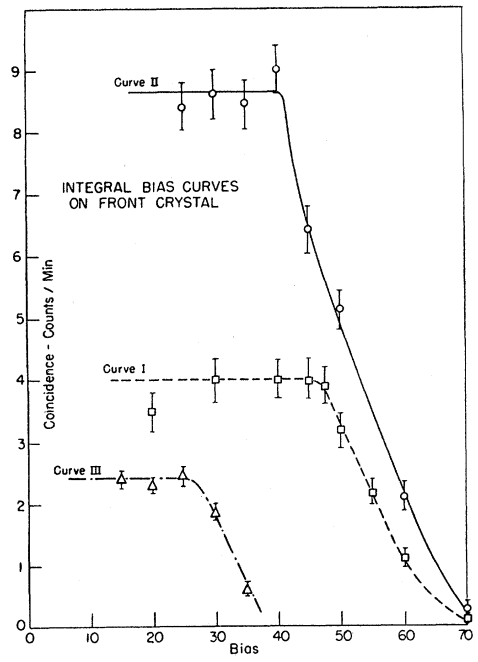

FIG. 4. Coincidence counting rate as a function of the bias on the front crystal. Curve I is for the back bias set close to the maximum for protons with no lead absorbers between crystals. Curve II is for the back bias set at a slightly lower value with no lead between crystals. Curve III is for the back bias set the same as in Curve II, but with a $\frac{1}{2}$-in. Pb absorber between crystals.

sponding to this geometry, are shown as broken curves in Fig. 1. The energy loss in the back crystal is scarcely altered by this modification, and the curve of energy loss in the front crystal is shifted in such a way as to make it essentially independent of absorber thickness.

These predictions have been checked for a number of absorber thicknesses and have been born out by the observations. The reasons that we have normally chosen to operate the telescope with the absorber between the crystals, despite the above mentioned disadvantage, are concerned with the elimination of spurious counts due to neutrons and mesons. Fast neutrons can produce protons in the material in front of the crystals or in the front crystal, and these protons will be counted provided that their energies lie in the range to which the telescope is sensitive. Placing the absorber in front of the telescope enhances the number of such spurious counts, both because of the increased thickness of material available for proton production and because the number of neutrons capable of producing protons of the requisite energy is greater, since the telescope itself is sensitive to lower-energy protons and neutrons, when the absorber precedes the front counter.

The problem of eliminating the background due to π mesons presents greater difficulties. These arise from the fact that a π meson which comes to rest in the back crystal gives rise to a larger pulse height than that which corresponds to its ionization energy loss. If it is positively charged, the decay μ^+ meson has an energy of 4.2 Mev and a very short range; its energy must be added to the energy loss of the π^+ meson. (The μ^+ meson decay, which gives rise to an electron of average energy $\sim$20 Mev, has a sufficiently long lifetime so that it does not add to the pulse height, provided that the detector resolving time is better than $\sim$1 μsec; the π^+ to μ^+ decay time cannot be resolved in a NaI:Tl crystal.) Negative π mesons are captured and give rise to nuclear disintegrations, which can add considerably to the energy losses (from ionization by the π^- meson alone) which are plotted in Fig. 2. Thus, it is possible for a π^- meson, of energy such that it barely penetrates into the back crystal, to trigger the telescope, even though the bias settings are such that it would not be detected if it behaved according to the curves of Fig. 2.

The difficulties arising from this possibility are especially serious in the proton energy range which we have investigated owing to the fact that the cross section for production of π mesons of energy capable of triggering the telescope is a number of orders of magnitude greater than that for the production of the high energy protons here under investigation. Thus, the rapid rise in the counting rates at the low bias settings, as seen in Figs. 3 and 4, can be accounted for by π-meson detection. Furthermore, the probability of counting a π meson is greater when the absorber is placed in front of the telescope than when it is placed between the two crystals, since the energy loss in the front crystal of a π meson which can just penetrate into the back crystal is sufficiently great in the first case to exceed the bias appropriate to the detection of protons. This is the main reason why we have preferred to place the absorber between the crystals.

A number of possibilities have been advanced for minimizing the spurious counts. One technique is to localize the end of the charged particle range by placing a third crystal, set in anticoincidence to the other two, at the back end of the telescope. This device eliminates those negative π mesons one of whose disintegration products penetrates into the anticoincidence crystal.

Another means of decreasing the π-meson background is by use of differential pulse-height analysis on either of the two crystals, or both. The main effect of this modification is to make more stringent the conditions under which a π meson can cause a count. Differential pulse-height analysis is most effective when used on the back crystal, since the additional energy loss due to the capture of negative π mesons is spread over a wide range of energies.

Most of the measurements, discussed in the next section have been made with a simple two-crystal telescope using integral pulse-height discrimination. The more recent measurements employed differential pulse-height analysis in the back crystal. However, a sufficient number of variations—in crystal thickness, position of the absorber, use of an anticoincidence crystal, use of differential pulse-height discrimination—have been tested so as to provide sufficient understanding of the workings of the proton telescope to determine those bias settings which minimize the background counting rates. Thus, we have good reason to believe that our measurements actually represent the fast photoprotons, with only a small fraction of possible neutron or π-meson contamination. Nevertheless, those data for which the counting rates have been especially small (mainly at the highest energies and largest angles) are still subject to a certain amount of uncertainty concerning the extent of the π-meson contamination. Fortunately, the main conclusions which can be drawn from the data are not seriously affected by these uncertainties.

Finally, in evaluating the data, it is necessary to know what fraction of the protons, which enter the telescope, are counted. Protons can be lost by suffering nuclear absorptions or scattering in the absorber, or by (multiple) Coulomb scattering in the absorber. This latter effect can be minimized by using an absorber of light material; we have used aluminum absorbers in some of our later measurements. In addition, the proton loss due to Coulomb scattering is decreased when the absorber is placed between the crystals of the telescope.[19] The

[19] One can avoid losses due to Coulomb scattering by employing a geometry in which as many protons are scattered into the detectors as are scattered out. We have tried to approximate such a geometry by using absorbers that extend beyond the crystals and which are as close as possible to the back crystal.

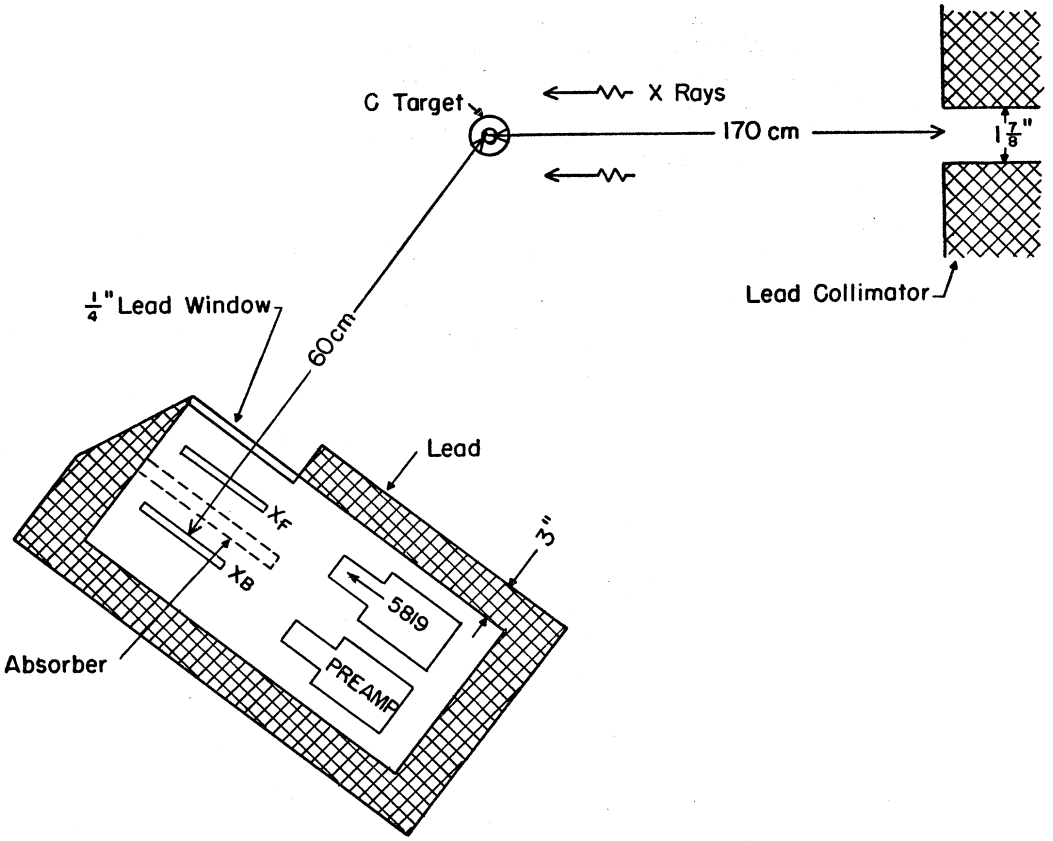

FIG. 5. Schematic drawing of angular distribution apparatus.

data can be corrected for the loss of protons due to nuclear interactions, provided the cross sections are known. We have assumed a nuclear cross section equal to the geometric value (with a radius $R=1.4A^{\frac{1}{3}}\times10^{-13}$ cm) in making this correction.

III. THE MEASUREMENTS

The geometrical arrangement for taking data is depicted in Fig. 5. The targets, which were in the form of cylinders or cylindrical shells, were centered in the x-ray beam with their axes vertical. The target cylinders were of sufficient height to extend over the entire vertical diameter of the (circular) beam and the target diameter was somewhat smaller than that of the beam which was $\sim$3 in. at the position of observation. The proton telescope was placed in a lead house on a turntable which could be rotated to any angle. This angle could be set to $\pm0.5°$ with respect to the beam direction.

This geometry has the advantage of cylindrical symmetry, thus insuring the reliability of angular distribution measurements. Its disadvantages lie in the difficulty of absolute cross-section measurements, since these depend on a determination of the average target thickness (which, together with the corresponding average proton energy loss in the target, was evaluated by graphical integration) as well as on a knowledge of the beam intensity and of its distribution over the area of the beam. However, the cylindrical geometry has been used only for relative cross-section measurements. The determination of the absolute cross section, at a single angle and energy, was achieved by use of a thin, plane target covering the entire area of the beam.

A. Carbon and Beryllium

The major fraction of our measurements were made with a carbon target, which was a cylindrical shell of 2-in. o.d. and $\frac{3}{8}$-in. thickness. The average energy loss of protons in the target, as computed from the range-energy relationships[18] by a graphical integration, were 12, 9.7, and 8.8 Mev for absorbers of 0 in., $\frac{1}{2}$ in., and 1 in., respectively, between the crystals (mean proton energies of 114, 159, and 194 Mev). Measurements at angles of 30° to the beam or greater were made with an angular resolution of $\pm5.4°$; at smaller angles, it was necessary to move the lead house further back, and the corresponding angular resolution was $\pm3.4°$.[20]

Measurements were also made with a Be target[21] of 2 in.-o.d. and $\frac{1}{2}$ in. thickness. These observations showed

[20] These figures include a spread of $\pm0.5°$ introduced by the finite size of the target.

[21] Kindly supplied by Professor A. Kaufmann of the M.I.T. Department of Metallurgy.

that, within the experimental accuracy of ~3 percent, the protons in a Be nucleus and in a C nucleus behave in an identical fashion with respect to high-energy γ rays—i.e., the angular distributions, for a given proton energy, are identical and the ratio of the cross sections of Be and C for the production of high-energy protons is 4:6. Hence, in the following discussions, the data obtained with the Be target have been combined with those obtained with the C target.

1. *Angular Distributions*

Careful measurements of the angular distributions of high-energy photoprotons have been made at three proton energies and at angles ranging from 20° to 160° in the laboratory frame of reference. The results are shown in Figs. 6–8. The limitations in the angular range resulted from the high background of electromagnetic radiation at the small angles, and from the low intensities of high-energy protons at the large angles. The errors plotted on the curves are entirely statistical and do not include provision for a mesonic background. The mesonic background could be important at the largest angles although even there, it is probably less than ~10 percent.

The observations at the various angles were made by taking short "runs" always "bracketed" by observations at 30°. This was done in order to eliminate the effects of drift in the electronic circuits and the consequent variations of the efficiency and energy resolution of the counter telescope.

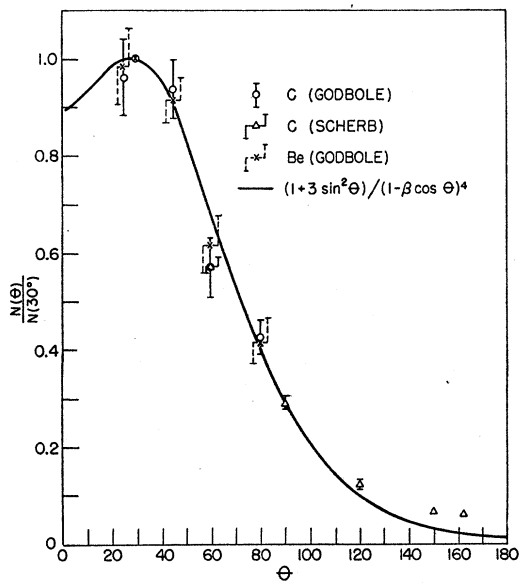

FIG. 6. The angular distribution in the laboratory of 126-Mev photoprotons from beryllium and carbon. The data marked "Scherb" were obtained at a later date than that marked "Godbole." The data are normalized to the value at 30°. The curve is a semiempirical fit to the data with $\beta=v/c$ of the protons.

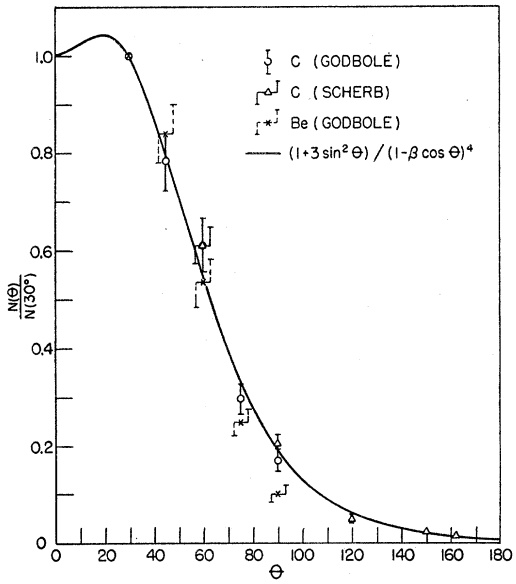

FIG. 7. The angular distribution in the laboratory of 169-Mev photoprotons from beryllium and carbon. The data marked "Scherb" were obtained at a later date than that marked "Godbole." The data are normalized to the value at 30°. The curve is a semiempirical fit to the data with $\beta=v/c$ of the protons.

The curves in Figs. 6–8 represent attempts to fit the data by a formula of the form

$$\frac{d\sigma/d\Omega}{d\sigma/d\Omega(30°)}=\frac{a+b\sin^2\theta}{(1-\beta\cos\theta)^4}, \tag{1}$$

where $\beta=v/c$ of the protons observed. This form, although suggested by the atomic photoeffect,[22] should be regarded in our case only as an empirical formula which provides a very good fit to the data over the range of observation with a relatively small variation with energy of the ratio $\alpha=b/a$. Its possible significance will be discussed in a following section.

2. *Energy Dependence at 30°*

In order to investigate carefully the energy dependence of the cross section for high-energy photoproton production, a separate run was made with the telescope at 30° to the beam. Special care was taken, in this run, to insure stability of the electronics and to evaluate the proton energy resolution of the telescope at each energy. Aluminum absorbers were employed, between the crystals of the telescope, to minimize the effects of multiple Coulomb scattering on the detector efficiency. The results of the run are shown in Table I. Columns 1 and 3 give the mean proton energies and energy spreads accepted by the telescope; these have been determined from curves similar to those shown in Fig. 1, computed for the various aluminum absorber

[22] A. Sommerfeld, *Atombau und Spektrallinien* (Friedrich Vieweg und Sohn, Braunschweig, Germany, 1939), Vol. 2, Chap. 6.

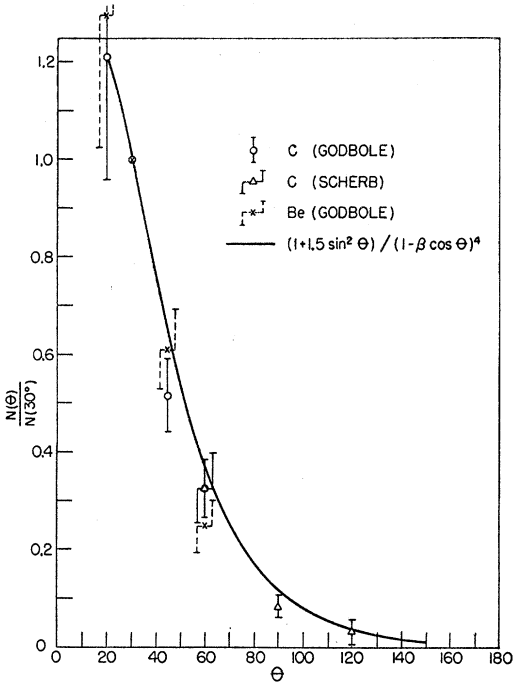

FIG. 8. The angular distribution in the laboratory of 203-Mev photoprotons from beryllium and carbon. The data marked "Scherb" were obtained at a later date than that marked "Godbole." The data are normalized to the value at 30°. The curve is a semiempirical fit to the data with $\beta=v/c$ of the protons.

thicknesses employed. Column 2 gives the observed ratios of the counting rates for the different aluminum absorber thicknesses to the counting rate for no absorber (average energy 126 Mev). Column 4 lists the corrections we have applied for the nuclear scattering and absorption of protons in the Al absorber, computed on the basis of an assumed constant (with energy) mean-free-path of 30 cm. The figures in column 5 represent the corrected ratios of the number of fast protons, per unit proton energy interval, to the number at 126 Mev. The errors given are purely statistical.

The results from column 5 of Table I are shown as a log-log plot in Fig. 9. It is seen that the number of protons falls off as $E^{-2.2}$ at the lower energies and as $E^{-7.6}$ at higher energies, with a relatively sharp break in the spectrum occurring at 193 Mev. The position of the break in the spectrum is, from these data, determined to within a few Mev.

The sharp break in the proton spectrum is in accordance with the "deuteron" model of Levinger.[13] At a laboratory angle of 30° and a maximum photon energy of 325 Mev, a static deuteron model would lead to a proton energy cutoff at 226 Mev. The cutoff becomes a break in the yield curve when account is taken of the motion of the nucleons inside a complex nucleus; however, this modification should not appreciably shift the position of the break. Nevertheless, the observed position of the break can be reconciled with the deuteron model provided it is assumed that our bremsstrahlung spectrum has actually started to fall off appreciably at ~300 Mev and, further, that the average proton has a binding of about ~15 Mev in a carbon nucleus. That this possible agreement may be somewhat fortuitous, will be seen in the subsequent discussion of Sec. IV B.

3. *Absolute Value of the Differential Cross Section*

In order to convert the relative cross-section measurements to absolute values, a measurement was made of the differential cross section for the production of 126-Mev protons at 45° to the beam. A thin plate of carbon, 1 cm thick, was mounted with its plane at 45° to the beam direction, so as to minimize the proton energy spread introduced by ionization energy loss in the target. The plate covered the entire area of the beam, thus allowing us to employ the beam calibration of Ratz.[23]

The value of the differential cross section obtained for the photoproduction by 325-Mev bremsstrahlung radiation per carbon nucleus of 126 Mev protons at 45° in the laboratory system is 0.40×10^{-30} cm²/Mev-steradian-Q.[24] The statistical uncertainty in this measurement is ±6 percent. However, the uncertainty of the calibration of the beam is considerably greater (as much as ~30 percent). Within these uncertainties the above value is in agreement with the value of 0.47×10^{-30} cm²/Mev-sterad-Q obtained by Keck[12] at the same angle and approximately the same energy.

Using the above value and the measured angular distribution, we obtain the values 0.45×10^{-30} cm²/Mev-sterad-Q for the differential cross section at 30°, and 2.22×10^{-30} cm²/Mev-Q for the total cross section for the production of 126-Mev protons from carbon by 325-Mev bremsstrahlung radiation.

B. Z Dependence

Previous investigators have observed[12,14] that, at least over the range of energies, angles, and targets

TABLE I. The spectrum of photoprotons from carbon at 30° from 325-Mev bremsstrahlung.

Mean energy of protons (Mev)	Observed ratio of the No. of protons at energy E to that at 126 Mev	Energy spread accepted by telescope	Fraction of protons detected	Corrected ratio of the No. of protons at E to that at 126 Mev
126	1.000	18.0	0.960	1.000
148	0.591 ±0.05	15.8	0.907	0.72 ±0.07
165	0.395 ±0.04 0.415 ±0.04	14.7	0.859	0.55 ±0.04
186	0.252 ±0.03 0.282 ±0.03	13.6	0.808	0.42 ±0.03
203	0.153 ±0.015	12.7	0.770	0.27 ±0.03
212	0.098 ±0.011	12.5	0.739	0.186 ±0.025
243	0.030 ±0.007	11.6	0.654	0.068 ±0.013

[23] H. Ratz, Massachusetts Institute of Technology Master of Science Thesis, 1952 (unpublished).

[24] One Q, or equivalent quantum, corresponds to 325 Mev of photon energy; i.e., the number of Q is the energy in the beam divided by the maximum photon energy. Thus, for a $1/E$ spectrum we have, for the number of quanta of energy E, $dN=QdE/E$.

studied, the cross section for fast photoproton production in a given element is essentially proportional to the number of protons Z in the nucleus. Our own observations on this question are in agreement with those of the others, so we shall confine ourselves to a brief summary of our results.

Mention has been previously made of the comparison between carbon and beryllium. This comparison is interesting mainly in that the identity of protonic behavior is established over a very wide range of angles and energies (see Figs. 6–8). However, the nuclei involved are not very dissimilar.

Another series of observations, made in the rather early stages of this investigation, is summarized in Fig. 10. In this comparison targets of three elements—carbon, aluminum, and iron—were compared at four settings (absorber thickness) of our proton telescope at an angle of 45°. The targets were made to have the same diameters and equal absorption for the high-energy photons [equal values of the number of atoms $\times Z(Z+1)$]. In order to achieve this, it was necessary to construct the Al and Fe targets in the form of thin wafers. Due to the decreasing mass of the higher-Z targets, the corrections for proton energy loss in the targets also decreased with increasing Z; hence the fact that the points for the different targets, at the same telescope setting, are plotted at different proton energies.

The significant feature of Fig. 10 is that all the points, when plotted as yields per proton, lie on the same smooth curve. While the accuracy of this comparison is not especially high, the range of energies covered is rather greater than that of the previous work. At the time this comparison was made, in the early stages of our work, our understanding of the workings of the proton telescope were not complete, so no particular significance should be attached to the exact shape, slope, etc., of the curve drawn in Fig. 10. However, it should be noted that, for instance, had the true dependence of the photoproton production been on the nuclear surface area rather than on Z, the points in Fig. 10 would have separated into three sets, one for each target, with the curve through the carbon set lying ~55 percent above that through the Fe set. Since indeed the cross section for charged photomeson production is more in proportion to the nuclear area than volume, the results shown in Fig. 10 helped to increase our confidence that the proton telescope was detecting mainly nucleons.

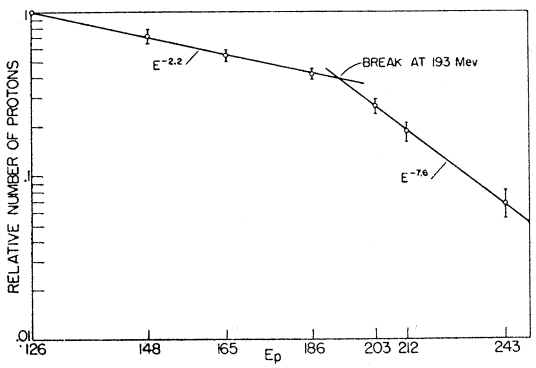

FIG. 9. The energy distribution of photoprotons from carbon at 30°. Both scales are logarithmic. The original data have been corrected for the attenuation in the telescope and the energy spread accepted by the telescope (see Table I). All the data are normalized to the value at 126 Mev.

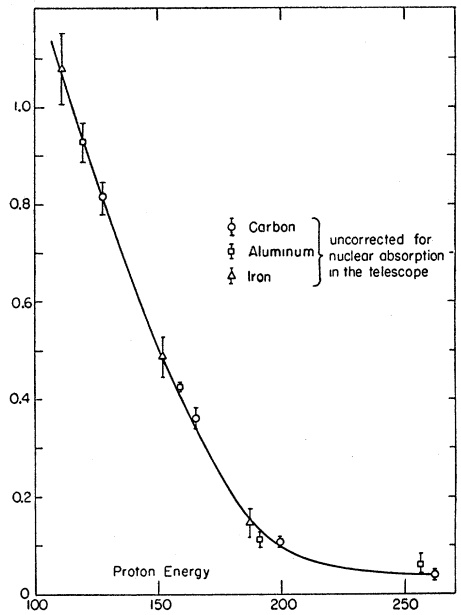

FIG. 10. The relative yields *per proton in the nucleus* of photoprotons from carbon, aluminum, and iron as a function of proton energy at 45°. Both scales are linear. The data are corrected for the energy spread accepted by the telescope but not for the attenuation in the telescope. (These are early data—see text.)

It should also be noted that these data are consistent with the linear dependence of the cross section on (NZ/A) which is predicted by the Levinger deuteron model;[13] the difference between a strict Z dependence and such a dependence would be only 7 percent for the case of a comparison of Fe and C targets.

IV. DISCUSSION

A. Comparison with Other Investigators

A detailed comparison with the results of other experiments in this field is difficult. Owing to the very rapid variation of the spectral properties with energy and angle, a slight difference in the conditions of angle or energy can lead to a large difference in the proton spectrum observed. In general, the various observations exhibit the same gross features, namely sharply forward-peaked angular distributions and power-law energy spectra; all the experiments show a break in the slope of the spectrum at some energy more-or-less consistent with the predictions of a deuteron model.

However, any attempt at a more critical comparison

TABLE II. Comparison of experiments on the spectra of high-energy photoprotons.

Observer	Max photon energy (Mev)	Lab. angle	Observed energy of break (Mev)	Predicted energy of break (Mev)	Observed slope below break	Observed slope above break
This paper	325	30°	193	211	2.2	7.6
This paper	325	45°	190	191	2.6	8.3
Rosengren and Dudley[a]	322	45°	140	189	1.7	3.0
This paper	325	60°	185	168	2.9	8.4
Keck[b]	320	67.5°	130	155	1.7	6
Rosengren and Dudley[a]	322	90°	140	122	1.7	4.4
This paper	325	90°	185	123	3.4	9.0
This paper	325	total	190	···	2.9	8.1

[a] See reference 14.
[b] See reference 12.

indicates that the situation, especially as regards comparison with the deuteron model, is still rather more confused than otherwise. Table II summarizes the results of the various investigators concerning the proton energy spectra (see Table II). Column 1 lists the observers, column 2 the maximum energy of the bremsstrahlung radiation used, and column 3 the angle of observation. Column 4 gives the energy at which the break in the proton spectrum was observed. (The observed values of lines 2, 4, 7, and 8—corresponding to the present paper—have been deduced from other observations, rather than measured directly, in a fashion to be described in the next section.) Column 5 lists the energies at which the break is predicted on the basis of a static deuteron model; the energies given are those corresponding to the maximum photon energy (column 2) minus 15 Mev for the nuclear binding. The last two columns list the observed slopes of the straight lines on log-log plots of the proton energy distributions below and above the "breaks" in the spectra, respectively.

It is clear from Table II that there exist serious discrepancies, both in the comparison with the predictions of the static deuteron model and the comparison between the various experiments. These discrepancies probably arise from a number of causes. In the first place, as has been discussed in Sec. II of this paper, the problem of eliminating completely the pi-meson background is quite difficult, especially at the higher proton energies or larger angles where the relative number of mesons incident on the telescope is exceedingly high. A small meson contamination in the highest-energy points can have a large effect, both on the energy of the "break" and on the slope of the curve above the "break." Since the techniques used by the various investigators, although similar in principle, differed in many details, the spurious backgrounds (probably small in all cases) could have been sufficiently different to account for some of the differences in the observed spectra.

However, even assuming ideal proton detection in all the experiments, the discrepancies of Table II could, in actual fact, be more apparent than real. Let us assume for instance that the proton spectrum does not, in fact, break sharply but, rather, has a monotonically increasing slope which changes most rapidly in the region of the "break" predicted by the static deuteron model.[25] The observed "breaks" might then simply result from the fact that a relatively small number of points have been recorded in each of the investigations, together with the desire of the investigators to represent the data in the form of straight lines on a log-log plot. It would also follow that the higher the energy range of the investigations the higher the apparent energy of the "break" and the greater the apparent slopes of the energy spectra, both below and above the "breaks." Since the measurements of this paper covered a range of higher energies than those of the previous investigations, this would help to account for some of the discrepancies observed in Table II.

However, the above considerations, while they may weaken the apparent contradictions between the various experiments, do not remove the most serious discrepancies between the observations and the "deuteron model," as will be seen in the following discussion.

B. Comparison with the Deuteron Model

There are essentially three aspects in which the experimental results have been compared with the model of Levinger,[13] in which it is assumed that the fast photoprotons originate from the photodisintegration of deuteron-like subunits within the nucleus. These are angular distributions, energy distributions, and total cross section. All of these have been touched upon in the preceding. However, these aspects are not unconnected, and it is of some interest to attempt to summarize the results of this comparison.

The angular distributions for 126-, 169-, and 203-Mev protons, plotted in Figs. 6–8, are quite different from those predicted in the paper of Levinger. The differences are manifest in two aspects: the positions of the maxima (if any) and the failure to observe a kinematical "cutoff."

According to Levinger, the angular distributions at the energies of our observations should show pronounced maxima in the region between 30° and 60°. According to our observations, the peaks (if they are there at all) lie well below 30° at all the energies of observation. However, as has been pointed out by Rosengren and Dudley,[14] this fact is not necessarily in contradiction with the deuteron model, since Levinger assumed a $\sin^2\theta$ angular distribution in the c.m. system for the deuteron photodisintegration; the assumption of a flatter or forward peaked distribution could move the peak sufficiently far forward to remove this discrepancy. Such a distribution is not excluded by the existing data on the photodisintegration of the deuteron.[26,27]

[25] Indeed the computations of Levinger (see reference 13), in which account is taken of the motion of the protons within the nucleus, point to just such a behavior.
[26] T. S. Benedict and W. M. Woodward, Phys. Rev. **85**, 924 (1952).
[27] W. S. Gilbert and J. W. Rosengren, Phys. Rev. **88**, 901 (1952).

The failure to observe a kinematical cutoff in the angular distributions is more difficult to reconcile with a deuteron model. For a static deuteron, the angular distributions plotted in Figs. 6–8 should cut off at ~90°, 60°, and 35°, respectively (account being taken of ~15-Mev binding per nucleon in the carbon nucleus). When consideration is given to the internal motion of nucleons within the nucleus, the kinematical cutoffs should at least manifest themselves by an abrupt change in the nature of the angular distributions above the angles, with the cross sections falling off much more rapidly beyond the cutoff angles. No such effect is observable in Figs. 6–8. Indeed, if anything, the data at 126 Mev indicate that the falloff is even less rapid than anticipated by the empirical relationship of Eq. (1).[28]

It might be argued that the more rapid decrease in the angular distribution for 203-Mev protons [$\alpha=1.5$ as compared to 3 for the lower energies, see Eq. (1)] is a manifestation of this effect. However, this change in the angular distributions is certainly considerably less striking than the effects predicted by the calculations of Levinger. Indeed, in order to reconcile our results with the deuteron model, it would be necessary to assume that the momentum distribution of the nucleons within a carbon nucleus contains a *very* large component of nucleons with relatively higher momenta than predicted by the Fermi distribution.

On the other hand, our energy distribution at 30° (Fig. 9) appears to manifest the expected kinematical cutoff, in a rather striking fashion, at a position more or less in agreement with the prediction of the deuteron model. This might be encouraging for the model, were it not for the fact, as seen in Table II, that this agreement does not carry over to other angles, when our observed angular distributions are taken seriously. This contradiction is made more clear by consideration of the curves in Fig. 11, from which the numbers exhibited in Table II have been extracted. The energy distributions plotted in Fig. 11, at 45°, 60°, 90°, and for the total cross section have been computed from the data at 30° (column 5 of Table I) and the assumption that the angular distributions are given by Eq. (1), with $\alpha=3$ for the four lower-energy points and $\alpha=1.5$ for the three high-energy points. However, points have also been plotted which were computed on the assumption of $\alpha=2$ at 186 Mev and $\alpha=1$ at 243 Mev, and it is clear that these alterations do not have a serious effect on the deduced energy distributions. It would appear difficult to reconcile these results with the deuteron model unless we are prepared to question the reality of the spectral break (as discussed, in the preceding section) and to assume that the dynamical effects of the internal motion of the nucleons within the nucleus

[28] However, a rough estimate of the effects of scattering within the carbon nucleus indicates that the empirical relationship may indeed fit well over the entire energy range (see reference 16).

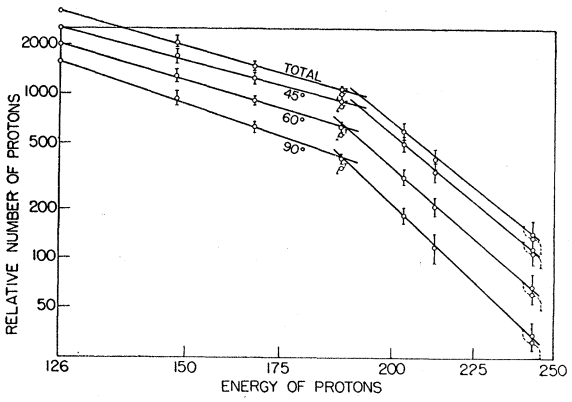

FIG. 11. Calculated energy distributions of photoprotons at various angles. Both scales are logarithmic. The relative number of protons at each angle is arbitrarily normalized to the value at 126 Mev. The values were computed from the data at 30° by means of the semiempirical formulas. The solid line points have a value of $\alpha=3$ from 126 Mev to 186 Mev and 1.5 from 203 Mev to 243 Mev. The dotted line points have a value of $\alpha=2$ at 186 Mev and a value of $\alpha=1$ at 243 Mev.

are considerably greater than indicated by the computations of Levinger.

It is perhaps of some interest, at this point, to remark once more on the empirical relationship, Eq. (1), which shows such surprisingly close agreement with the angular distribution data. Since this formula has been adopted from the atomic photoelectric effect, it is tempting to conclude that its applicability is evidence that we are dealing with a direct nuclear photoeffect. This conclusion is, however, for the time being unwarranted, since there does not exist a theory of the nuclear photoeffect at these energies. Nevertheless, it must be admitted that the authors find the suggestion difficult to avoid.

However, if we were indeed observing a direct nuclear photoeffect, we might also expect that the angular distributions of the emitted protons would depend on the states of initial angular momentum of the protons within the nucleus. It was for this purpose that we undertook a rather careful comparison between the angular distributions from beryllium and carbon, with the result that we were unable to observe any difference. Since, according to the shell model, the ratio of protons in a p state to those in an s state is 1:1 in Be and 2:1 in C, a difference of the type noted above might have been quite marked. These observations, then, would seem to indicate that we are not dealing with a direct photoeffect.

The absolute cross section for the production of 126-Mev protons (Sec. III A.3) is also quite large as compared to what would be expected on the basis of a direct photoeffect. Thus, if we neglect the nuclear recoil, the cross section per 126-Mev photon would be $126\times2.22\times10^{-30}$ cm^2 or 2.8×10^{-28} cm^2.

On the other hand, assuming a deuteron model, 126-Mev protons at 30° would result from photons of

$\sim$200 Mev, and the corresponding differential cross section for the photodisintegration of the deuteron would be $\sim 1.5\times 10^{-29}$ cm^2/steradian, which is not inconsistent with the direct observations.[26,27]

C. Conclusions

The measurements described in the preceding were intended to provide a quantitative check on the deuteron model of Levinger[13] for the photoproduction of high-energy protons from complex nuclei. The results, however, remain rather ambiguous. They provide a partial confirmation on the basis of the general features of the energy distributions and the absolute cross section, while at the same time indicating apparent contradictions on the basis of the angular distributions. These contradictions may be a result of inadequate theoretical treatment of the momentum distribution of the protons within the carbon nucleus.

However, some of the contradictions indicated in the preceding may result from experimental difficulties, which should certainly be investigated further. In addition, it seems evident that a direct proof of the deuteron hypothesis, in the form of observation of the simultaneous emission of a neutron and a proton together with measurements of their angular correlations, would be highly desirable. More careful measurements of the energy distributions at various angles, to establish definitely the existence and the position of a kinematical cutoff, are also necessary before more precise conclusions can be drawn from the data. These problems are receiving further attention in our laboratory.

Finally, provided that a model for the origin of the high-energy photoprotons can be definitely established, accurate measurements of the type outlined above should provide useful information concerning the momentum distributions of nucleons within complex nuclei.

The authors wish to thank Professor P. Morrisson for his valuable discussions. We are very grateful to Professor W. L. Kraushaar for much of the electronic equipment employed in these measurements. It is also a pleasure to thank the members of the synchrotron staff and especially J. S. Clark for the many hours which were contributed to these experiments.